energies

MDPI

Article

Improving the Efficiency of Environmental Temperature Control in Homes and Buildings

Murat Kunelbayev [1,*], Yedilkhan Amirgaliyev [1] and Talgat Sundetov [2]

[1] Institute of Information and Computer Technologies, Al Farabi Kazakh National University, Almaty 050040, Kazakhstan
[2] Institute of Information and Computer Technologies, International Information Technology University, Almaty 050000, Kazakhstan
* Correspondence: murat7508@yandex.kz

Abstract: This research developed an effective environmental temperature control system for homes and buildings. The study used a photovoltaic panel (PV) and developed a solar installation with thermosiphon circulation, which has a flat solar collector and heat-insulating translucent glass with double glazing with reduced pressure. The coolant is made of thin-walled corrugated stainless pipe. The heat from the solar flux heats the liquid removed from the collector, and cold water from the siphon enters its place. There is a constant circulation of heat, which increases heat transfer efficiency by eliminating additional partitions between the panel and thermal insulation. We have also developed a solar system control controller, which includes an electronic unit with six sensors. The six sensors are controlled by the STM32 programmable Logistics Integrated circuit (FPGA), designed to monitor the entire solar system, and the drives include power relays. The performance of the photovoltaic panel and the room's temperature change are calculated during both the simulation and testing of the controller. The standard error was 20% compared to other controllers. During the experiment, the consumption savings amounted to about 1% due to the control signal in the controller, which has a significant impact on the service life of the equipment.

Keywords: photovoltaic panel; flat solar collector; control controller; sensors; temperature control in buildings

Citation: Kunelbayev, M.; Amirgaliyev, Y.; Sundetov, T. Improving the Efficiency of Environmental Temperature Control in Homes and Buildings. *Energies* **2022**, *15*, 8839. https://doi.org/10.3390/en15238839

Academic Editor: Luisa F. Cabeza

Received: 23 August 2022
Accepted: 9 November 2022
Published: 23 November 2022

1. Introduction

The research in [1] developed intelligent homes and buildings that are becoming a reality with the functions of connection and integration into the ecosystem, as well as improvements in the quality of life of users, comfort, safety, and security while increasing the efficiency of resource use. In [2], a control system for smart homes was developed, which allowed household appliances to increase efficiency. The article [3] describes a system for reducing the approximate amount of load on consumed energy in the United States. In the study [4], controllers were developed that are necessary to maintain the ambient temperature within a desired temperature profile. In addition, in this article, the authors mentioned that controllers could be open and closed. In the paper [5], a method for temperature control and energy accounting in low-temperature heating systems is presented. The paper [6] presents an extensive overview of climate control. In [7], proportional-integral regulators were developed that evaluate the efficiency of residential buildings. In [8], the main parameters of a solar collector with thermosiphon circulation for a solar heat supply system are considered. In the research [9], a system was proposed that reads the temperature in the rooms from the available power supply. The authors of [10] present an overview of buildings' energy consumption and comfort management systems. Issues regarding comfort, energy supply, and the controller are considered, and control systems and their shortcomings are discussed. The architecture of a multi-agent control system used to improve the energy efficiency and comfort of a building is presented, and

a new paradigm in information technology, ambient Intelligent, is mentioned. Ambient Intelligent is a new approach to creating an intelligent environment. In [11], the authors developed an economic model predictive control (MPC) method that can be used in combination with thermal energy storage (TEC) to temporarily shift energy consumption from periods of high demand to periods of low energy cost. Additionally, based on convex optimization, a new controller design has been developed that controls many of the behaviors observed in the case of a finite horizon and also significantly reduces the computational effort required for the operation. In [12], a new simulation environment is presented, resulting from the merger of City Sim, an energy-building simulator, and Tensor Flow, a powerful machine learning library. The new simulation environment has the potential to develop building energy scenarios in which machine learning algorithms such as deep reinforcement learning are applied to critical challenges and opportunities facing modern cities, such as increased demand for heating and cooling due to population growth.

The paper [13] demonstrated a new approach based on deep learning that can eliminate the appearance of static pressure in sensors. An LSTM-based model has been used that studies static pressure over time to eliminate the static pressure sensor from the system. It has been experimentally confirmed that, regardless of the seasonal characteristics and performance of the power supply system, the proposed model can match the static pressure measured by the sensor. In [14], the authors developed a fuzzy logic controller (FLC) applicable to various plant sizes. Design principles have been applied for a controlled environment that can mimic the behavior of a CSC over a wide range of system sizes. By regulating one additional input, the controller provides users with a compromise between power consumption and control accuracy. Simulations were run using the same FLC in the greenhouse and broiler house. The article [15] developed a new genetic algorithm with actual code for a self-tuning fuzzy logic control (PLC) with temperature in a greenhouse, in which the arithmetic crossover operator and the replay operator based on ranking are adapted. Compared to the primary systems, the proposed VLC fuzzy control system provides higher performance in terms of improved control accuracy and energy savings. For prediction, the authors considered the influence of incident solar radiation, wind speed, and outdoor temperature. The proposed methods were evaluated only by modeling using MATLAB Simulink 7.*/R2006/2007. In the research [16], a combination of the concept of fuzzy logic and neural networks was developed, in which an adaptive neuro-fuzzy controller was introduced to adjust the internal temperature of the greenhouse, testing the method with a complex dynamic model of the environment using the MATLAB Simulink environment. In the research [17], an approach using the series is applied to develop a nonlinear model predictive controller for the nonlinear dynamics of a greenhouse environment. Developing a thermodynamic model for the internal environment is not an easy task. In the paper [18], models were developed based on the energy balance equations of interfaces (such as windows, floors, walls, and ceilings) that form the boundaries of the internal environment. However, to be effective, this method requires the precise determination of many parameters, such as the coefficient of thermal resistance of surfaces, which are difficult or even impossible to obtain. In the articles [19–21], alternative approaches, including finite element analysis, were used—as they often are—to study the energy efficiency of buildings.

This study aimed to improve the efficiency of environmental temperature control in homes and structures. A solar energy and heat supply system was developed, a photovoltaic panel (PV) was used, and a solar installation with thermosiphon circulation was developed. They were presented on an exact deployed installation.

2. Materials and Methods

The developed master control of the solar thermal system is able to measure the characteristics of a thermal solar installation with a chemical coating, which can be compared with similar characteristics of a traditional two-circuit solar installation with a thermosiphon. Figure 1 shows the solar thermal system.

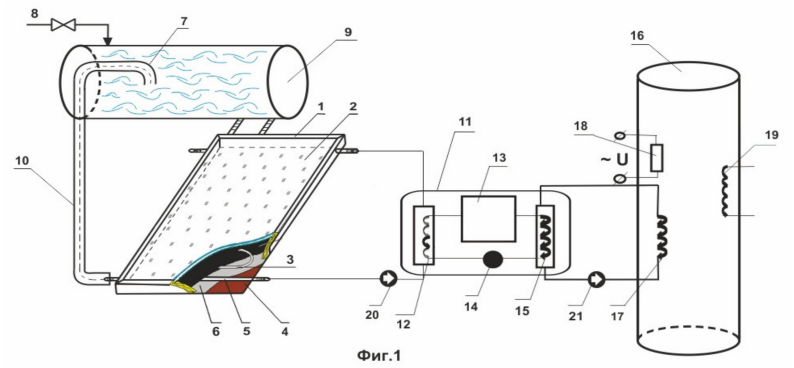

Figure 1. Solar thermal system with thermosiphon.

In the above figure, 1 is a flat solar collector; 2, a translucent insulating transparent double-glazed window; 3, a coil; 4, the bottom of a flat solar collector; 5, inlet and outlet pipes; 6, a heat insulating film; 7, a siphon dispenser tank; 8, a pipeline with a valve for cold water; 9, a dispenser tank; 10, a circulation pipe; 11, a heat pump; 12, an evaporator; 13, a compressor; 14, a valve; 15, a condenser; 16, a heat exchanger of the heating system; 17, an electric drive; 18, a backup electric heater; 19, a heat exchanger of the heating system; and 20 and 21, circulation pumps.

In this section, we will study dependencies sufficient for the more complex models mentioned above to be easy to model, since the nonlinearities of the circuit, ultimately leading to instability, are aggravated so that an implementation controlled by the equations of the system is adopted [22]. The dynamic model equations are:

$$\left(\frac{\partial T_{heater}}{\partial t}\right) = \left(\frac{T_{heater_{avg}}}{\tau_{heater}}u - \frac{1}{\tau_{heater}} * T_{heater}\right) \quad (1)$$

$$\left(\frac{\partial Q}{\partial t}\right)_{heater} = (T_{heater} - T_{room}) * M_{dot} * c \quad (2)$$

$$\left(\frac{\partial Q}{\partial t}\right)_{losses} = \frac{T_{room} - T_{out}}{R_{eq}} \quad (3)$$

$$\left(\frac{\partial T_{room}}{\partial t}\right) = \frac{1}{M_{air} * c} * \left(\frac{\partial Q_{heater}}{\partial t} - \frac{\partial Q_{losses}}{\partial t} + S_{rad} * W_{area}\right) \quad (4)$$

where $\partial Q/\partial t$ is the heat flow from the heater into the room (W/m^2); c is the heat capacity of the air at constant pressure (J/(kg·K)); $M_{\dot{dot}}$ is the mass flow of air through the heater (kg/s); T_{heater} is the temperature from the heater (°C); $T_{heater_{avg}}$, average heater temperature (°C); τ_{heater}, heater time constant (s); T_{room}, current indoor air temperature (°C); T_{out}, outdoor air temperature (°C); M_{air}, indoor air mass (kg/s); R_{eq}, equivalent thermal house resistance (K/W); S_{rad}, solar radiation (W/m^2); and W_{area}, total window area (m^2).

2.1. Thermosiphon Solar Water Heater

A single-circuit solar water heater with a thermosiphon multilayer stationary reverse flow circuit, which is divided by several perpendiculars, is solved using the Bernoulli equation applied to the supply circuit:

$$\Delta P_i = \rho_i * g * \Delta h_i + \rho_i * g * h_{Li} \quad (5)$$

This model includes a velocity satisfying the calculated friction pressure of the fluid in the collector and a separate insignificant capacity

$$T_{po} = T_a + (T_{pi} - T_a)\exp[-\frac{(UA)_p}{mC_p}] \quad (6)$$

The friction pressure loss in the pipe is defined as

$$H_p = \frac{f * L * v^2}{2d} + \frac{Kv^2}{2} \tag{7}$$

$$T_{ck} = T_a + \frac{I_T F_R(\tau\alpha)}{F_R U_L} + (-T_a - \frac{I_T F_R(\tau\alpha)}{F_R U_L}) * \exp[\frac{F' U_L}{G * C_p} * \frac{\left(k - \frac{1}{2}\right)}{N_x}] \tag{8}$$

The amount of heat in the system is:

$$Q_u = r_c A(F_R(\tau\alpha) I_T - F_R U_L(T_{CI} - T_a) \tag{9}$$

where

$$r_c = \frac{F_{R,use}}{F_{R,test}} = \frac{G(1 - \exp(\frac{U_L \dot{F}}{G C_p})}{G_{test}(1 - \exp(\frac{U_L F}{G_{test} C_p})} \tag{10}$$

2.2. The Battery Tank

The average temperature supplied for loading is:

$$T_d = \frac{V_h T_h + (V_L - V_h) T_1}{V L} \tag{11}$$

The calculated conductivity of the storage tank is:

$$\rho C_p V_i \frac{dT_i}{dt} = -(UA)_i(T_i - T_{env}) + (k_S A)_{i-1} \frac{(T_{i-1} - T_i)}{\Delta h_{i-1}} - (k_s A)_i \frac{(T_i - T_{i+1})}{\Delta h_{i+1}} \tag{12}$$

$$Q_{in} = m_h C_p(T_h - T_R) \tag{13}$$

The amount of the substance is:

$$Q_{sup} = m_L C_p(T_D - T_L) \tag{14}$$

In [23], a system for combined thermal/light modeling and CFD modeling has been developed. The residential building shown in Figure 2a,b was used for this purpose.

(**a**) (**b**)

Figure 2. Photovoltaic panel (**a**) A building used to evaluate a temperature control system; (**b**) a photovoltaic panel used to measure solar radiation.

The size of the room: length, 10 m; width, 9 m; height, 3 m; window area = 80 m^2; wall area, 0.105 m^2. Technical characteristics: maximum heating temperature, 70 °C; heating power, 8000 watts.

Figure 3 shows a full-scale model for achieving this goal, which we have developed in principle. On the basis of this model, various types of solar systems will be created in accordance with the size and design used for water heating and room heating.

Figure 3. Layout of the heat collector.

Figure 4 shows a thermal installation, which consists of an air-water heat pump, a circulation pump for circulating liquid through the system, as well as an expansion tank and a storage tank.

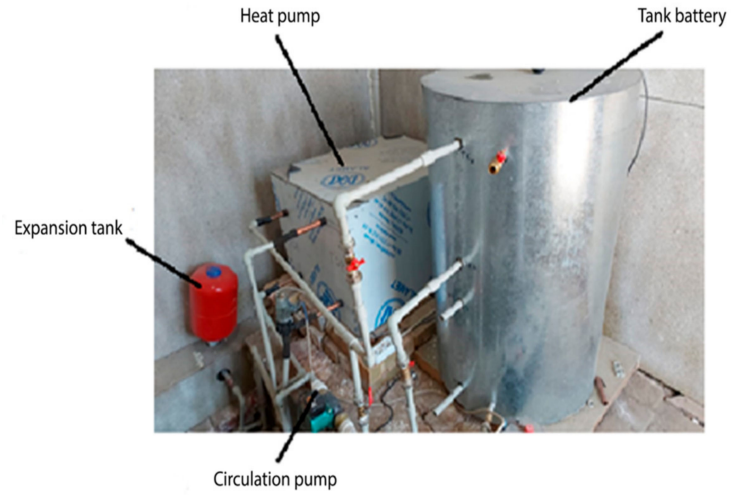

Figure 4. Thermal installation.

In general, the translucent glazing of the solar installation is reduced, and there is also a coolant pipe. Water from the flat solar collector of the siphon takes its place, removing heat and eliminating the partitions of the thermal energy panel. Water from a flat solar collector enters a circulation pump—a household appliance for pumping liquid. An electric motor and a working shaft are installed in the housing. When turned on, the rotor begins to rotate the impeller, which creates reduced pressure at the inlet and increased pressure at the outlet. The circulating water enters the spiral-to-spiral heat exchanger in the intensity region, after which the water is pumped into the storage tank. There is also an expansion tank—an element of the heating system designed to receive excess water from its thermal expansion due to heating.

In [24], the influence of the façade features of the building on heat loss was developed, and the reduction of heat loss due to passive energy-efficient solutions was estimated in

order to preserve the appearance of the façade. It is able to provide an accurate estimate of the amount of solar radiation with a much smaller achievement of this goal generated by the panel at the moment. It is necessary information to have a calibration value from the reference pyranometer to obtain constant efficiency of the panel.

The novelty in the study is based on the management of the house. In this study, improving the efficiency of environmental temperature control in homes and buildings is an auxiliary tool that eliminates nonlinear fluctuations, allowing one to use a simpler solution to track performance. Benchmarks tests are carried out in the same climatic conditions, for one day, in a period ranging from 12 to 15 h, when the air temperature and intensity of solar radiation are the most stable.

This study is a solar energy system control controller that includes an electronic unit with six sensors controlled by a programmable logistics integrated circuit (FPGA) STM32 designed to monitor the entire solar energy system, and the actuators include power relays. The ESP 32 module receives temperature data and synchronizes with six sensors connected to the STM32 FPGA, with six electrical wires programmed in C++; the data is received by the clock in real-time. After the entire process is completed, all sensor data is transferred to the ESP 32 module and stored in the database.

The control controller has a programmable logistics integrated circuit STM32, which is connected to six digital sensors (temperature, water flow, pressure, heater tank coolant temperature, heat exchanger coolant temperature, and outdoor temperature) and to a built-in software real-time measuring device. The built-in real-time measuring software is connected to an ESP32 module and four valves. The operation of the entire system is displayed on the display.

The work of the proposed controller is carried out as follows.

Six digital sensors (temperature sensor, water flow sensor, pressure sensor, coolant temperature sensor in the heater tank, coolant temperature sensor in the heat exchanger, and outdoor temperature sensor) register the temperature of a flat solar collector. Six sensors are controlled by a programmable logic integrated circuit STM32. Temperature records are stored on the ESP32 module, which in turn sends temperature readings and valve states every 5 s. In the built-in software, the real-time measuring device records the date and time of temperature data measurements, sending them to the programmable logistics integrated circuit STM32. Each of the six sensors is connected to the STM32, with six electrical wires, programmed in C++, so that after processing the temperature, date, and time data received from the built-in software measuring in real time, respectively, in the ESP32 module. Temperature data, date, time, and valve states of the system and the selected mode of operation of the solar energy system are displayed on the display.

3. Results

Experimental tests were carried out without interruption from 7:30 to 19:30 in static mode (without inflow and outflow of water from the tank), absorbing incident solar radiation. After 19:30, during the drain mode (or dynamic mode), the water was drained through the outlet at a constant flow rate. The proposed measurement technique took place on a farm. Every 15 min, the data acquisition system registered the temperature distribution in charging mode and every 15 s in discharge mode. In dynamic mode (drain), cold water from the upper tank entered a flat solar collector with a thermosiphon. A proportional amount of hot water collected at the outlet served household needs. The drain mode continued until the hot water temperature dropped to 30 °C. For simplicity, the initial temperature was set to 30 °C, which is close to the peak ambient temperature at the current location during charging.

The angle of inclination of the flat solar collector was chosen equal to $\beta = 45^{\circ}$ since the city of Almaty is located in the center of the Eurasian continent, in the southeast of the Republic of Kazakhstan, at 43° north latitude. Therefore the optimal location of the angle of inclination of the collector would be about 45°, but if we use collectors all year round, it is recommended to choose the angle of inclination of a collector to the horizon

15° less than latitude. In our case, it was about 45°. It can also be said that if the actual orientation of the solar collector on the object differed less than 15° on the horizon from the zero orientation to the astronomical south, then the losses would not be so great. However, if it were technically impossible to implement these requirements, then the efficiency of solar systems would fall, and investments in them would never pay off.

The effective angular zone of operation for flat and vacuum tubular collectors is about 45° in each direction from the perpendicular to the surface, that is, in total, about 90°, and the total solar radiation on the inclined surface was set as Gg = 750 W/m^2. The outside wind speed was set to w = 2.5 m/s, and the ambient temperature was 20 °C.

The tests were carried out with a clear, cloudless sky and a total solar radiation flux density of at least 600 W/m^2. The outside air temperature was at least 15 °C.

The following additional devices were used in the testing process:

- pyranometer M-80 paired with a secondary device
- cup anemometer.

The automatic wireless weather station Vantage Vue was used, which provided accurate and reliable weather monitoring, as well as continuously recorded meteorological data at regular intervals (every 60 s) using the Weather-Link program controlled by a PC-based system. The ambient temperature recorded by the weather station had an accuracy of 0.5 °C. The industry standard pyranometer measures incident solar radiation with a nominal accuracy of 5 W/m^2.

The wind speed during the collector tests was not to exceed 5 m/s. Wind speed measurements were to be carried out in the immediate vicinity of the collector at a height corresponding to half the height of the collector.

The tests were carried out at a water flow rate through the collector of 25 kg/(m^2·h) and a water temperature at the inlet to the collector of 20, 30, 40, and 50 °C. The water temperature was changed from test to test. Thus, at least 4 tests were to be carried out. The duration of the tests was at least 2 h. Five thermocouples were connected to a data monitoring system that measured the temperature at various points within the system.

The experimental studies on a photovoltaics panel used an ammeter and a DC voltmeter, a multimeter UT206, an oscilloscope, and a switch.

Figure 5 shows the temperature trends from the panel tanks and the data for four days—from 15 to 27 June 2022.

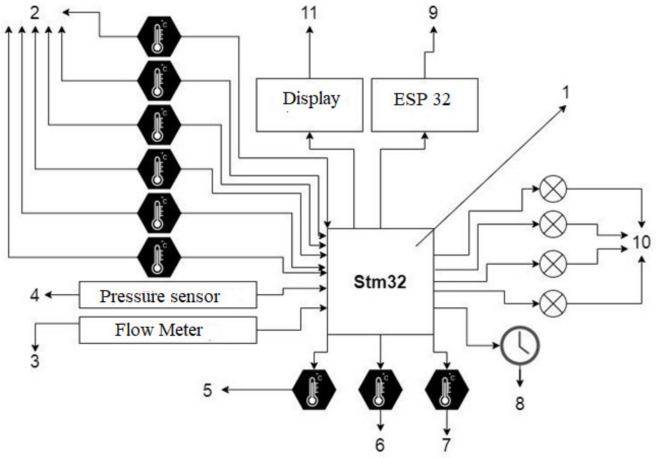

Figure 5. Block diagram for the control controller. (**1**) programmable logistics integrated circuit; (**2**) temperature sensor; (**3**) water flow sensor; (**4**) pressure sensor; (**5**) coolant temperature sensor in the heater tank; (**6**) coolant temperature sensor in the heat exchanger; (**7**) outdoor temperature sensor; (**8**) built-in software measuring device real-time; (**9**) ESP32 module; (**10**) four valves; (**11**) operation display.

Figure 6 shows the control controller for the solar heat supply system.

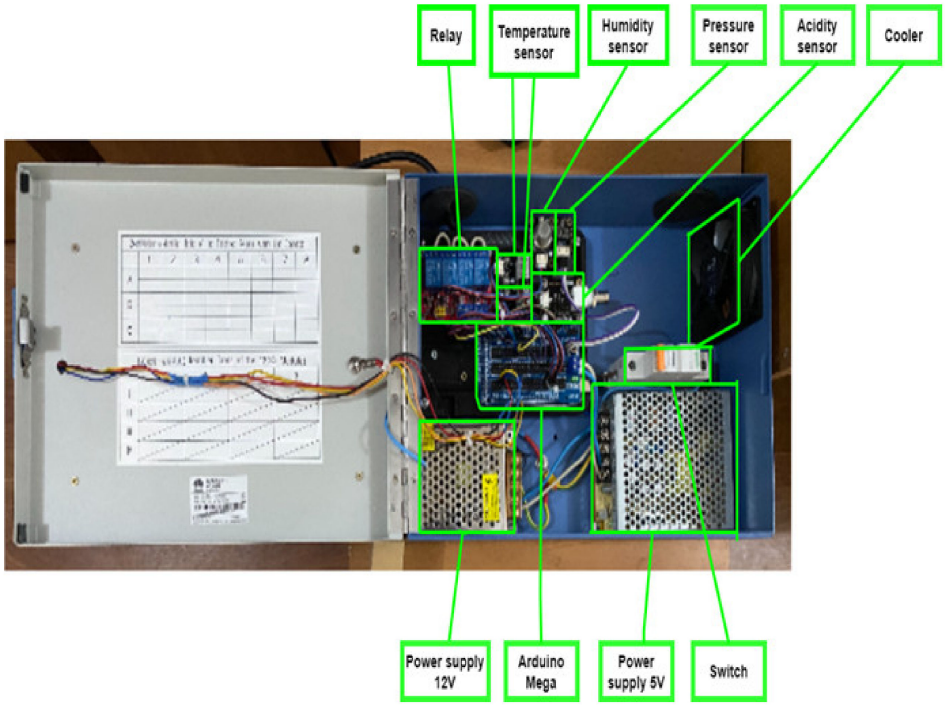

Figure 6. Photo of the controller with the cover removed.

Figure 7 shows the verification of temperature sensors using an infrared pyrometer with 300-3 "Photon".

Figure 7. Checking temperature sensors using an infrared pyrometer with 300-3 "Photon".

Figure 8 shows a cup anemometer for measuring wind speed.

Figure 8. Cup anemometer.

Figure 9 shows an experimental stand for research on a photovoltaic panel.

Figure 9. In experimental studies on the photovoltaic panel.

Figure 10 shows the temperature dependence on the day and time. This dependence shows how the temperature of the solar heat supply system in the summer period changes over time. As you can see from this figure, the air temperature is high in summer, the temperature of the flat solar collector rises, and the temperature in the heat exchanger is low due to the pressure drop and the high coefficient of solar radiation, since the installation is located in the south.

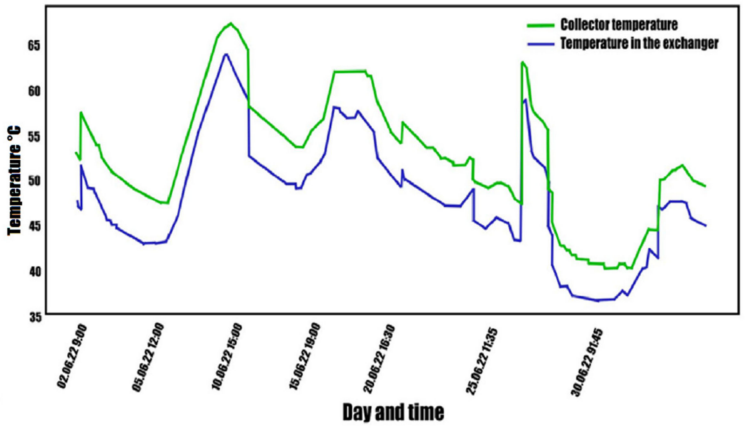

Figure 10. Temperature dependence on day and time.

Figure 11 shows the characteristics of the photovoltaic panel after calibration, an example of the measurements carried out. During the experimental work, a time interval was chosen to change the usual drops at 6:00 pm.

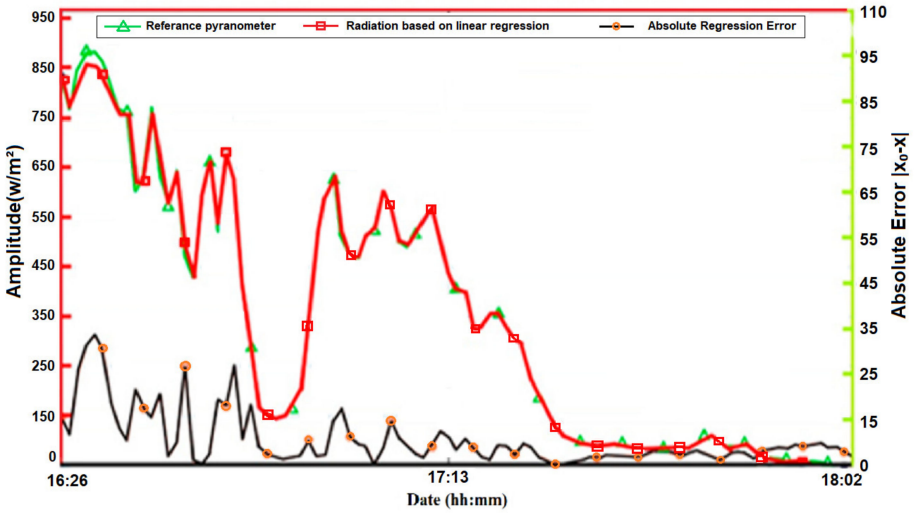

Figure 11. Photovoltaic panel performance.

In [25,26], a model is presented for predicting indoor temperature and energy consumption from the electric heating of the premises in an office building using stochastic differential equations. This article [27] discusses working with solar energy. On the basis of generalizing data on the duration and daily movement of distribution volumes for June and December in the territory as "technically applicable and economically profitable solar energy," this concept was developed. This paper [28] presents the optimal management of renewable energy in a green building using powerful reinforcement learning for electricity management. In article [29], a mathematical model was developed, and the effect of temperature and radiation on the performance of a photovoltaic system was investigated. In [30], the immersion of a part in the formation of water was investigated. In the research for [31], the author investigated the construction and efficiency of solar hot water heating systems. The geometry and dimension of a solar energy system were defined based on the material's thermal properties. In the research for [32], the authors proposed using the algorithms for the calibration of small solar hot water heating systems and the application in MatLab.

Thermal performance is calculated based on the first law of thermodynamics (energy), but that does not allow for estimating a flat solar collector [33]. The second law of thermodynamics (exergy) estimates the various losses in the flat solar collector and allows for estimating a solar hot water heating system [34,35]. The authors [36] used the numerical inverse Laplace homotopy technique for solving some interesting 1-D time-fractional heat equations. The authors of [37] have provided the numerical arrangement of ordinary differential equations (ODE) that appeared from different problems; in the simulation of a solar hot water heating system, decreasing the simulation time can be considered. In [38], the author provided analytical and numerical techniques for physical fields in the physical time domain; the problems that appeared in a solar hot water heating system due to the mechanical deformation during the thermal gradient temperature were applied on the outer surface. In paper [39], the authors presented isotherms, streamlines, local Nusselt numbers, global Nusselt numbers, and global fluid temperatures numerically and graphically.

In Kazakhstan, there is extensive attention to developing a solar hot water heating system. The system's price is high; therefore, it is unavailable for all customers. The new hybrid energy system with mathematical methods, computer simulation, software, and hardware help optimize the price of flat solar water heating systems. One way to efficiently use energy is to use a new source of energy (renewable and environmentally friendly) in

Kazakhstan's fuel and energy system. Thus, the development of an energy system based on the double-circuit solar system with a heat pump is an actual and urgent problem for autonomous power supply. Kazakhstan has a high potential for the generation of solar energy. The simulation was performed for different temperature conditions and levels of solar irradiance for the Almaty region. The simulation process was done in MatLab and Simulink, a tool often used for other simulation processes and, in particular, for the simulation of solar hot water heating systems [40,41]. Using the simulation, we evaluated the technical possibility of a solar water heating system and indicated the system nodes to be modified and improved for Kazakhstani weather conditions. As a result of the numerical simulation used in the control system was obtained using MATLAB. The dynamic action of the modification of the building was carried out together with the use of a set of Simulink tools based on a constant period modification adopted with thermodynamic equations. The results of reservoir simulation showed that the heat sink coefficient increased with increasing collector size. This dependence was closer to the thickness of the collector than to the surface area of the collector. The surface area of the absorber plate could affect the absorption of heat. The higher the average temperature of the absorber plate, the higher the absorption coefficient. Thus, a collector with a larger surface area will transmit a greater amount of incident thermal radiation. In addition, for a collector with large dimensions, the overall heat transfer coefficient is greater.

Figure 12 shows a step-by-step evaluation of the dynamic model. As can be seen from this figure, the evaluation using the dynamic model of the basic approximation seems to be the best way to approximate the effect of room temperature when controlling the degree of heating capacity. The required selection time can be freely extracted from the data shown in this figure. To be able to use the controller implementation, one needs to show the necessary poles of the isolated circuit. The use of a continuous, isolated system leads to a good compromise between performance and efficiency.

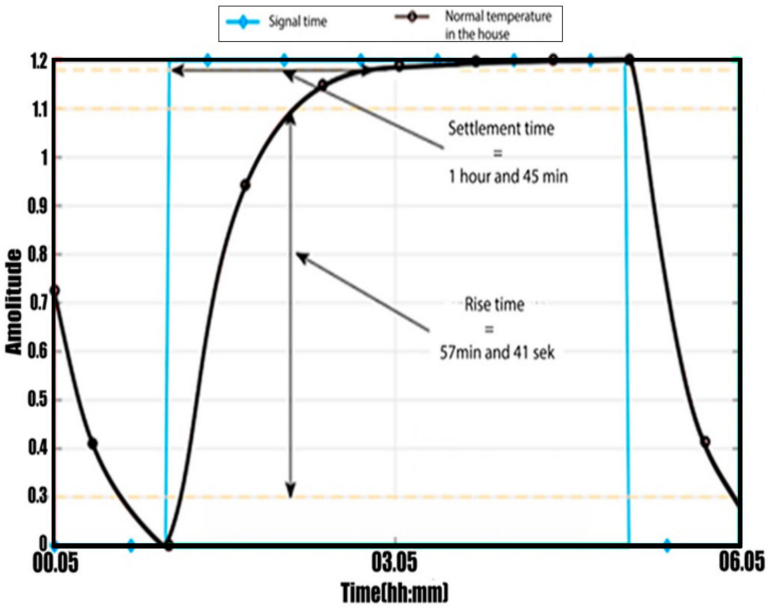

Figure 12. Step-by-step response of the dynamic model.

Figure 13 shows the change in room temperature during controller simulation. As one can see from this figure, the controller only works on the current room temperature to decide whether to turn the heating system on or off when the room temperature changes around the selected set point. In the controller, the input signals are extended to correct the last room temperature and the last applied control signal, taking into account external interference, namely the incident solar radiation and the ambient temperature.

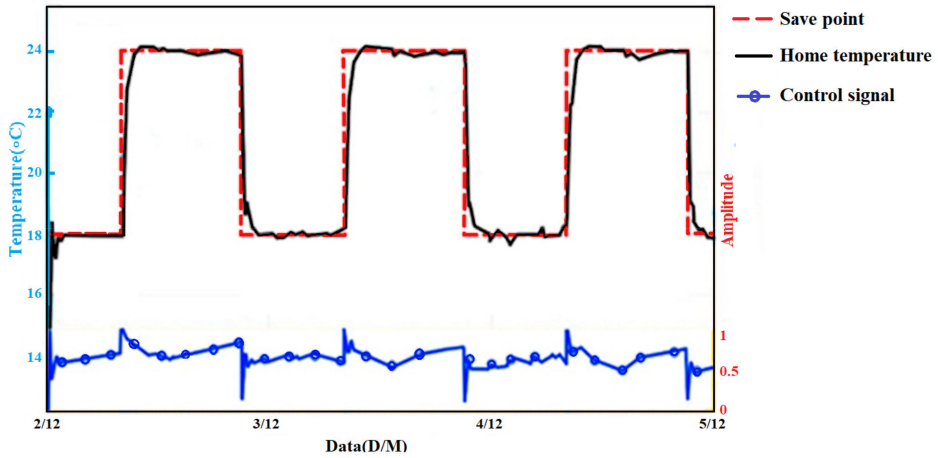

Figure 13. Room temperature change during simulation for the controller.

Figure 14 shows the environmental conditions during the simulation and shows that a simpler controller causes fluctuations with a significant change in environmental conditions.

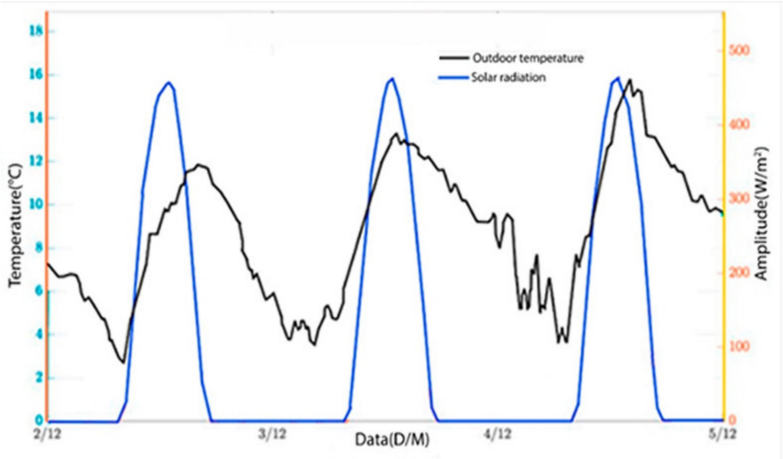

Figure 14. Environmental conditions during simulation.

Figure 15 shows the temperature change in the room and the control signal applied to the heating system associated with the set value. The set value is tracked with good accuracy.

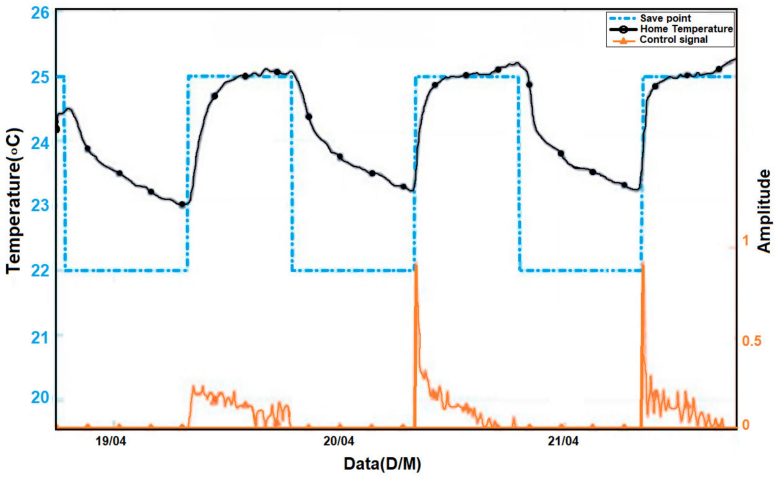

Figure 15. Room temperature change during controller test.

It can also be said that Figures 14 and 15 show more straightforward implementations of the controller, which lead to more significant fluctuations at times when environmental conditions change significantly. This phenomenon is due to the incorrect estimation of the coefficients of the first-order model since it is impossible to separate the change in solar radiation and outdoor temperature from the change in the heating system. Conversely, in the extended implementation of the controller, this situation does not arise since the regression vector has more parameters, which provides more flexibility to separate the influence of solar radiation conditions from turning on heating towards changing the temperature in the room.

4. Discussion

Experiments were conducted with the controller to obtain comparable data. Qualitatively, the practical results correspond to the simulation results. The controller is highly sensitive to incident solar radiation, demonstrating sharp and significantly large temperature fluctuations. The standard error was 20% compared to other controllers. During the experiment, the consumption savings amounted to about 1%, significantly impacting energy consumption and the equipment's service life. The operating costs were also estimated, showing an improvement of about 7% compared to the other controller. The experimental results relate to specific measurements taken on different days and under different conditions, so they should be carefully reviewed. Nevertheless, they provide clear indications that using this controller in combination with external variables is effective compared to other controllers. Unlike others, the developed controller can be implemented with minimal additional costs, so the benefits largely compensate for the additional complexity.

5. Conclusions

This study used a new design of the control controller in houses with ambient temperature. The performance of the photovoltaic panel was calculated after calibration. Experimental studies of the measurements were used in the summer from 8:00 to 19:00. The article also presents an experimental installation with the regular use of a thermal collector. Fluctuations between constraints led to a decrease in the performance of the controller. An increase in system performance due to the introduction of a more advanced controller was beneficial. In the future, they will be evaluated using predictive functions, which may be intervals of work. While this approach improves productivity by using long-term data, integrating various variables with forecasts is challenging, especially when dealing with highly dynamic scenarios, such as buildings subject to changing usage patterns. In addition, the system performance will also be evaluated with other types of drives. In the course of future work, the performance of other controller algorithms will be evaluated, namely algorithms with forecasting functions that can cover longer time intervals in advance so that weather forecasts can influence the management strategy. The goal here is to investigate how well the controller training process works in the face of actual types of drives that have heterogeneous characteristics, for example, radiant floors that have only heating capabilities and exhibit slow response and air conditioning devices that can heat and cool the internal environment and receive an almost instantaneous response. This is a practical but essential aspect that needs to be carefully studied to determine how widespread this approach is and what benefits are obtained on a case-by-case basis.

6. Patents

1. Patent for Invention of the Republic of Kazakhstan. Dual-circuit solar unit with thermosiphone circulation. N° 33741. Date of registration 2 July 2019. Invertors: Amirgaliyev Yedilkhan, Murat Kunelbayev, Auelbekov Omirlan, Nazbek Katayev, Aliya Kalizhanova, Ainur Kozbakova.

2. Patent for Utility Model of the Republic of Kazakhstan. Control controller of solar system. N° 4012. Date of registration 28 May 2019. Amirgaliyev Yedilkhan, Murat Kunelbayev, Auelbekov Omirlan, Nazbek Katayev, Aliya Kalizhanova, Ainur Kozbakova.

Author Contributions: Conceptualization, M.K.; methodology, Y.A.; software, T.S. All authors have read and agreed to the published version of the manuscript.

Funding: This research has been funded by the Science Committee of the Ministry of Science and Higher Education of the Republic of Kazakhstan, Grant AP 14871625, BR18574144.

Conflicts of Interest: The authors declare no conflict of interest.

References

1. Chan, M.; Campo, E.; Estève, D.; Fourniol, J. Smart homes—Current features and future perspectives. *Maturitas* **2009**, *64*, 90–97. [CrossRef] [PubMed]
2. Belic, F.; Hocenski, Z.; Sliskovi, D. HVAC control methods—A review. In Proceedings of the 2015 19th International Conference on System Theory, Control and Computing (ICSTCC), Cheile Gradistei, Romania, 14–16 October 2015; pp. 679–686.
3. Kavalionak, H.; Carlini, E. An HVAC Regulation Architecture for Smart Building Based on Weather Forecast. In *Economics of Grids, Clouds, Systems, and Services, Proceedings of the GECON 2018, Pisa, Italy, 18–20 September 2018*; Lecture Notes in Computer Science; Springer: Cham, Switzerland, 2018; Volume 11113.
4. Fontes, F.; Antão, R.; Mota, A.; Pedreiras, P. Adaptive Ambient Temperature Control of Indoor Environments. In Proceedings of the IECON 2019—45th Annual Conference of the IEEE Industrial Electronics Society, Lisbon, Portugal, 14–17 October 2019; pp. 255–260.
5. Rekstad, J.; Meir, M.; Kristoffersen, A. Control and energy metering in low temperature heating systems. *Energy Build.* **2003**, *35*, 281–291. [CrossRef]
6. Chinnakani, K.; Krishnamurthy, A.; Moyne, J.; Gu, F. Comparison of energy consumption in HVAC systems using simple ON-OFF, intelligent ON-OFF and optimal controllers. In Proceedings of the 2011 IEEE Power and Energy Society General Meeting, Detroit, MI, USA, 24–28 July 2011; pp. 1–6.
7. Wang, J.; Zhang, C.; Jing, Y. Application of an intelligent PID control in heating ventilating and air-conditioning system. In Proceedings of the 2008 7th World Congress on Intelligent Control and Automation, Chongqing, China, 25–27 June 2008.
8. Yedilkhan, A.; Murat, K.; Beibut, A.; Aliya, K.; Ainur, K.; Timur, M.; Azhibek, D. Mathematical justification of thermosyphon effect main parameters for solar heating system. *Cogent Eng.* **2020**, *7*, 1851629. [CrossRef]
9. Al-Ali, A.R.; Tubaiz, N.A.; Al-Radaideh, A.; Al-Dmour, J.A.; Murugan, L. Smart grid controller for optimizing HVAC energy consumption. In Proceedings of the 2012 International Conference on Computer Systems and Industrial Informatics, Sharjah, United Arab Emirates, 18–20 December 2012.
10. Dounis, A.; Caraiscos, C.; Caraiscos, C. Advanced control systems engineering for energy and comfort management in a building environment—A review. *Renew. Sustain. Energy Rev.* **2009**, *13*, 1246–1261. [CrossRef]
11. Mendoza-Serrano, D.I.; Chmielewski, D.J. HVAC control using infinite-horizon economic MPC. In Proceedings of the 2012 IEEE 51st IEEE Conference on Decision and Control (CDC), Maui, HI, USA, 10–13 December 2012; pp. 6963–6968.
12. Vázquez-Canteli, J.; Ulyani, S.; Kampf, J.; Nagya, Z. Fusing Tensor-Flow with building energy simulation for intelligent energy management in smart cities. *Sustain. Cities Soc.* **2019**, *45*, 243–257. [CrossRef]
13. Son, J.; Hyogon, K. Sensorless Air Flow Control in an HVAC System through Deep Learning. *Appl. Sci.* **2018**, *9*, 3293. [CrossRef]
14. Chao, K.; Gates, R.S.; Sigrimis, N. Fuzzy logic controller design for staged heating and ventilating systems. *Trans. ASAE* **2000**, *43*, 1885–1894. [CrossRef]
15. Xu, F.; Chen, J.; Zhang, L.; Hongwu, Z. Self-tuning Fuzzy Logic Control of Greenhouse Temperature using Real-coded Genetic Algorithm. In Proceedings of the 9th International Conference on Control, Automation, Robotics and Vision, Singapore, 5–8 December 2006.
16. Mohamed, S.; Hameed, I.A. A GA-Based Adaptive Neuro-Fuzzy Controller for Greenhouse Climate Control System. *Alex. Eng. J.* **2018**, *57*, 773–779. [CrossRef]
17. Atia, D.; El-madany, H. Analysis and design of greenhouse temperature control using adaptive neuro-fuzzy inference system. *J. Electr. Syst. Inf. Technol.* **2017**, *4*, 34–48. [CrossRef]
18. Gruber, J.; Guzmán, J.; Rodríguez, F.; Bordons, C.; Berenguel, M.; Sánchez, J. Nonlinear MPC based on a Volterra series model for greenhouse temperature control using natural ventilation. *Control Eng. Pract.* **2011**, *19*, 354–366. [CrossRef]
19. Piñon, S.; Camacho, E.; Kuchen, B.; Pena, M. Constrained predictive control of a greenhouse. *Comput. Electron. Agric.* **2005**, *49*, 317–329. [CrossRef]
20. Coelho, J.P.; Oliveira, P.B.M.; Cunha, J.B. Greenhouse air temperature predictive control using the particle swarm optimisation algorithm. *Comput. Electron. Agric.* **2005**, *49*, 330–344. [CrossRef]
21. Arvanitis, K.G.; Paraskevopoulos, P.N.; Vernardos, A.A. Multirate adaptive temperature control of greenhouses. *Comput. Electron. Agric.* **2000**, *26*, 303–320. [CrossRef]
22. North, G.R.; Cahalan, R.F.; Coakley, J.A. Energy balance climate models. *Rev. Geophys.* **1981**, *19*, 91–121. [CrossRef]
23. Clarke, J. *Energy Simulation in Building Design*; Routledge: London, UK, 2001.
24. Mortarotti, G.; Morganti, M.; Cecere, C. Thermal Analysis and Energy-Efficient Solutions to Preserve Listed Building Facades: The INA-Casa Building Heritage. *Buildings* **2017**, *7*, 56. [CrossRef]
25. Thavlov, A.; Bindner, H. Thermal Models for Intelligent Heating of Buildings. In Proceedings of the International Conference on Applied Energy, Suzhou, China, 5–8 July 2012.

26. Merembayev, T.; Amirgaliyev, Y.; Kunelbayev, M.; Yedilkhan, D. Thermal loss analysis of a flat plate solar collector using numerical simulation. *Comput. Mater. Contin.* **2022**, *73*, 4627–4640. [CrossRef]
27. Amirgaliyev, Y.N.; Wójcik, W.; Kunelbayev, M.; Merembayev, T.; Yedilkhan, D.; Kozbakova, A.; Auelbekov, O.; Kataev, N. Theoretical prerequisites of electric water heating in solar collector-accumulator. *News Natl. Acad. Sci. Repub. Kazakhstan Ser. Geol. Tech. Sci.* **2019**, *6*, 54–63. [CrossRef]
28. Wang, L.; Zhang, G.; Yin, X.; Zhang, H.; Ghalandari, M. Optimal control of renewable energy in buildings using the machine learning method. *Sustain. Energy Technol. Assess.* **2022**, *53*, 102534. [CrossRef]
29. Ghodusinejad, M.; Ghodrati, A.; Zahedi, R.; Yousefi, H. Multi-criteria modeling and assessment of PV system performance in different climate areas of Iran. *Sustain. Energy Technol. Assess.* **2022**, *53*, 102520. [CrossRef]
30. Elminshawy, N.; Osama, A.; Naeim, N.; Elbaksawi, O.; Tina, G. Thermal regulation of partially floating photovoltaics for enhanced electricity production: A modeling and experimental analysis. *Sustain. Energy Technol. Assess.* **2022**, *53*, 10258. [CrossRef]
31. Maldonado, R.D.; Huerta, E.; Corona, J.E.; Ceh, O.; Leon, A.I.; Henandez, I. Design and construction of a solar flat collector for social housing in México. *Energy Procedia* **2014**, *57*, 2159–2166. [CrossRef]
32. Nogueira, C.; Vidotto, M.; Toniazzo, G.; Debastiani, G. Software for designing solar water heating systems. *Renew. Sustain. Energy Rev.* **2016**, *58*, 361–375. [CrossRef]
33. Farahat, S.; Sarhaddi, F.; Ajam, H. Exergetic optimization of flat plate solar collectors. *Renew. Energy* **2009**, *34*, 169–1174. [CrossRef]
34. Luminosu, I.; Fara, L. Determination of the optimal operation mode of a flat solar collector by exergetic analysis and numerical simulation. *Energy* **2005**, *30*, 731–747. [CrossRef]
35. Park, S.; Pandey, A.; Tyagi, V.; Tyagi, S. Energy and exergy analysis of typical renewable energy systems. *Renew. Sustain. Energy Rev.* **2014**, *30*, 105–123. [CrossRef]
36. Yavuz, M.; Özdemir, N. Numerical inverse Laplace homotopy technique for fractional heat equations. *Therm. Sci.* **2017**, *22*, 185–194. [CrossRef]
37. Mahdy, A.; Youssef, M. Numerical solution technique for solving isoperimetric variational problems. *Int. J. Mod. Phys.* **2021**, *32*, 2150002. [CrossRef]
38. Mahdy, A.; Lotfy, K.; Hassan, W.; El-Bary, A. Analytical solution of magneto-photothermal theory during variable thermal conductivity of a semiconductor material due to pulse heat flux and volumetric heat source. *Waves Random Complex Media* **2021**, *31*, 2040–2057. [CrossRef]
39. Fayz-Al-Asad, M.; Yavuz, M.; Alam, M.N.; Sarker MM, A.; Bazighifan, O. Influence of fin length on magneto-combined convection heat transfer performance in a lid-driven wavy cavity. *Fractal Fract.* **2021**, *5*, 107. [CrossRef]
40. Morini, G.; Piva, S. The simulation of transients in thermal plant. Part I: Mathematical model. *Appl. Therm. Eng.* **2007**, *27*, 2138–2144. [CrossRef]
41. Morini, G.; Piva, S. The simulation of transients in thermal plant. Part II: Applications. *Appl. Therm. Eng.* **2008**, *28*, 244–251. [CrossRef]